2-1-2002

A Motor and a Brake: Two Leg Extensor Muscles Acting at the Same Joint Manage Energy Differently in a Running Insect

Anna N. Ahn
Harvey Mudd College

Robert J. Full
University of California - Berkeley

The Journal of Experimental Biology 205, 379–389 (2002)
Printed in Great Britain © The Company of Biologists Limited 2002
JEB3995

A motor and a brake: two leg extensor muscles acting at the same joint manage energy differently in a running insect

A. N. Ahn* and R. J. Full

Department of Integrative Biology, University of California at Berkeley, Berkeley, CA 94720-3140, USA

*Present address: Concord Field Station, Harvard University, Old Causeway Road, Bedford, MA 01730, USA (e-mail: aahn@oeb.harvard.edu)

Accepted 16 November 2001

Summary

The individual muscles of a multiple muscle group at a given joint are often assumed to function synergistically to share the load during locomotion. We examined two leg extensors of a running cockroach to test the hypothesis that leg muscles within an anatomical muscle group necessarily manage (i.e. produce, store, transmit or absorb) energy similarly during running. Using electromyographic and video motion-analysis techniques, we determined that muscles 177c and 179 are both active during the first half of the stance period during muscle shortening. Using the *in vivo* strain and stimulation patterns determined during running, we measured muscle power output. Although both muscles were stimulated during the first half of shortening, muscle 177c generated mechanical energy (28 W kg^{-1}) like a motor, while muscle 179 absorbed energy (–19 W kg^{-1}) like a brake. Both muscles exhibited nearly identical intrinsic characteristics including similar twitch kinetics and force–velocity relationships. Differences in the extrinsic factors of activation and relative shortening velocity caused the muscles to operate very differently during running. Presumed redundancy in a multiple muscle group may, therefore, represent diversity in muscle function. Discovering how muscles manage energy during behavior requires the measurement of a large number of dynamically interacting variables.

Key words: muscle, electromyography, work loop, neural control, locomotion, biomechanics, insect, arthropod, *Blaberus discoidalis*, cockroach.

Introduction

By measuring muscle length changes and forces *in vivo* during locomotion or under *in vivo* conditions, individual locomotor muscles have been found to have functionally diverse roles. Pectoral muscles in flying birds, the abductor muscle in swimming scallops, and myotomes in fish clearly generate power like a motor (Abraham and Loeb, 1985; Johnston, 1991; Biewener et al., 1992; Marsh et al., 1992; Rome et al., 1993), as do the ankle extensors of cats during running (Walmsley et al., 1978; Gregor et al., 1988; Prilutsky et al., 1996). In contrast, the leg muscles of hopping wallabies and running turkeys generate force nearly isometrically to perform little work during level running (Roberts et al., 1997; Biewener et al., 1998). The mechanical function of the turkey gastrocnemius changes depending on the incline of the running surface (Roberts et al., 1997). While the turkey leg muscle contracts isometrically when generating force on the level, it shortens considerably to generate mechanical work and power when the animals runs up a 12 ° incline. Moreover, a hindlimb extensor muscle in the cockroach may play a role in control by generating larger forces during lengthening and actively absorbing mechanical energy to slow leg movement during running (Full et al., 1998). Energy absorption, storage, and transmission also occur in flying and swimming animals, despite the large overall power demands of these activities. For example, locomotor muscles in flies absorb energy to control steering (Tu and Dickinson, 1994). In some fish, the cranial muscle fibers shorten early in a tail-beat to produce power that is transmitted by more caudal muscle fibers that do not themselves generate net mechanical energy (van Leeuwen et al., 1990; Altringham et al., 1993). These studies demonstrate the challenge in predicting the mechanical function of an individual muscle (for a review, see Dickinson et al., 2000).

The realization that individual muscles can function as motors, brakes, springs or struts during locomotion presents the possibility that muscles of a single anatomical group may not necessarily share the load or even share a common mechanical function. It is most often assumed that synergistic muscles share the work or load because muscles within a multiple muscle group are capable of executing the same action. *In vivo* studies show that the multiple ankle extensors in the cat and the wallaby operate together to share the force and power demands during locomotion (Walmsley et al., 1978; Abraham and Loeb, 1985; Prilutsky et al., 1996; Biewener et al., 1998). Numerous studies have modeled the functions of multiple muscles using assumptions of equal load-sharing (Seireg and Arvikar, 1975; Crowninshield, 1978; Dul et al.,

1984; Davy and Audu, 1987; Herzog and Leonard, 1991). Variation in function among muscles of a common anatomical group to generate coordinated movement is seldom considered a possibility.

For muscles of the same anatomical group to function similarly, one might expect the muscles to have similar intrinsic and extrinsic properties. Although many factors determine muscle force and power output during cyclical contractions (for a review, see Josephson, 1999), in the present study, we focus on three muscle properties: the kinetics of force generation, force–velocity relationships, and history-dependent effects. The twitch kinetics of a muscle are often tuned to the cycle frequency at which the animal locomotes. A muscle with faster twitch durations will generate maximum power at higher cycle frequencies, whereas a muscle with slower twitch durations will generate maximum power at lower cycle frequencies (Rome et al., 1988; Johnson et al., 1993; James et al., 1995; James et al., 1996; Swoap et al., 1993). At higher cycle frequencies, a muscle with faster twitch kinetics can generate force during muscle shortening, then relax before lengthening begins (Marsh, 1990; Johnson et al., 1993; Coughlin et al., 1996; Swank et al., 1997). A muscle with slower contraction kinetics tends to absorb energy at higher operating frequencies because its twitch duration exceeds the shortening period of the muscles (Caiozzo and Baldwin, 1997). Moreover, muscles operating on different regions of their force–velocity curves are more likely to manage energy differently (Biewener and Gillis, 1999). A muscle operating at approximately one-third of its maximum contraction velocity (V_{max}) tends to maximize power, whereas a muscle contracting near its V_{max} tends to generate lower forces and reduced power output (Curtin and Woledge, 1988; Rome et al., 1988) (for a review, see Josephson, 1993). History-dependent effects of muscle activity can also influence muscle function: shortening-induced force depression tends to reduce the work and power output of muscles undergoing large strains during cyclic contractions (Edman, 1975; Josephson, 1997; Askew and Marsh, 1998; Josephson and Stokes, 1999).

In the present study, we ask whether individual muscles within an anatomical muscle group necessarily function similarly during locomotion. We define muscle function as a muscle's ability to produce, store and return, or absorb mechanical energy over a cycle. We compare two of the six muscles (muscles 177c and 179, using the notation of Carbonell) (Carbonell, 1947), that can generate extensor moments at the coxa–femur joint of the cockroach hindlimb. One of the two muscles (muscle 179) is already known to absorb mechanical energy under *in vivo* running conditions (Full et al., 1998). Here, we ask whether both extensors share the load and function to absorb energy during running. To test the hypothesis of common mechanical function, we determined the strain and activation patterns of muscles 177c and 179 during running at the preferred speed. We then imposed cyclic *in vivo* strain and stimulation patterns on semi-isolated muscle while measuring force to determine work and power (Josephson, 1985a). Next, we explored the mechanisms responsible for the similarities or differences in function by measuring twitch kinetics and force–velocity relationships. We replicated the *in situ* energy measurements for muscle 179 under *in vivo* conditions to provide a direct and complete comparison of its function with that of muscle 177c. We selected these hindlimb extensor muscles because both muscles are parallel-fibered, are a single motor unit, lack inhibitory innervation, and act at a joint with a single degree of freedom.

Materials and methods

Animals

Cockroaches, *Blaberus discoidalis* (Serville), were obtained as adults from a commercial supplier (Carolina Biological Supply Co., PO Box 187, Gladstone, OR 97027, USA). The cockroaches were maintained in the laboratory in large, closed containers where they had free access to food (dried dog food) and water. The muscles selected for study, 177c and 179 of the hindlimb, using the notation of Carbonell (1947), are positioned to extend the coxa–trochanter–femur joint and depress the femur (Fig. 1). Muscle 177c inserts on an apodeme that attaches to the most proximal tip of the trochanter and is common to all the 177 muscles; it originates on the basalar (wing hinge). Although muscle 177c is biarticular, spanning both body–coxa and coxa–femur joints (Fig. 1), it functions only at the coxa–femur joint during running. Not only is the change in body–coxa angle during running very small (–8 ° during stance) (Kram et al., 1997), but muscle 177c also crosses the axis of rotation of the coxa–body joint. Therefore, muscle 177c only extends the coxa–femur joint and is

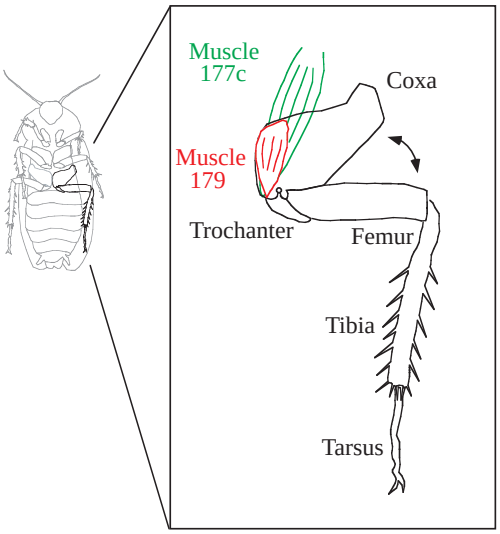

Fig. 1. Ventral view of the cockroach *Blaberus discoidalis*. The inset represents the left hind limb and muscles 177c and 179. Muscle 177c inserts on the medial tip of the trochanter and originates on the basalar plate (wing hinge). Muscle 179 inserts on the trochanter and originates on the ventral side of the coxa. The open circle indicates the axis of rotation of the coxa–trochanter–femur joint.

functionally monoarticular during running (Fourtner and Randall, 1982). Muscle 179 inserts on a small apodeme that extends from the anterior and proximal end of the trochanter and originates on the anterior wall and anterior coxal rim. Both muscles are innervated by single excitatory motor neurons (Pipa and Cook, 1959), with no inhibitory innervation (Pearson and Iles, 1971).

Seventeen males and twenty-six females (mass 3.20±0.82 g; N=43 animals; mean ± S.D.) were used in the experiments.

Electromyography and kinematics

Electromyographic (EMG) activity patterns from both muscles (177c and 179) were acquired during free running on a Plexiglas track. Simultaneously, we videotaped, from underneath, the clear track with a high-speed video camera system at 500 frames s^{-1} (Redlake Camera Systems, MotionScope) to determine the two-dimensional joint kinematics as the animals ran at their preferred speed. White spots (Liquid Paper) were painted with a pen onto the head, tail and hindlimb joints. We marked the body–coxa, coxa–femur, femur–tibia and tibia–tarsus joints and the pre-tarsal claws of both hindlimbs. Joint angles were calculated from the digitized points (Peak Performance Technology, Motus) for each run. The joint angles were then filtered with a third-order, low-pass Butterworth filter with a cut-off frequency of 25 Hz, determined by residual analysis (Biewener and Full, 1992).

For the EMG recordings, bipolar electrodes were made from 50 μm diameter (44 gauge) silver wire insulated with polyurethane (California Fine Wire) (for details, see Full et al., 1998). Each electrode was heated to form a small ball (Full et al., 1998). The ends of the electrodes were inserted into small holes in the basalar plate for muscle 177c and in the ventral, exoskeletal surface of the coxa for muscle 179. Inserted electrodes were fixed in place using dental wax. All wires were braided together to prevent electrical crosstalk and to form a convenient tether, which was waxed onto the pronotum. Muscle action potentials recorded from the running animals were amplified 100 times at a bandwidth of 3 Hz to 1 kHz (Grass P5 series a.c. pre-amplifiers) (Full et al., 1998) and were acquired at 3 kHz (Labview DAQ system; NI PCI-1200 boards) on a computer (Macintosh Power PC 9500/132). EMG signals were filtered with a second-order, high-pass Butterworth filter with a cut-off frequency of 100 Hz. We ensured the absence of crosstalk between the muscles and between the wires inserted into the muscles by using behaviors that resulted in muscle action potentials from one muscle, but not the other. During tethered flight trials, the animal activated muscle 177c, but not 179. During slow runs, the animals activated muscle 179, but not 177c. After the recordings, the animals were fixed in 70 % ethanol. Electrode placement was re-checked by careful dissection after fixation of the animals.

The animals ran at their preferred speed along a Plexiglas track (9 cm×66 cm) at room temperature (23 °C). Trials during which the animal ran straight at a steady speed and did not bump into the walls were accepted. Ten trials were obtained from six animals. Two consecutive cycles from each trial were analyzed (20 cycles in total). Six animals were used to determine the kinematic and electromyographic variables.

Muscle strain during running

The kinematics of the hindlimb determined during the videotaped EMG trials were played into a three-dimensional musculo-skeletal model of the cockroach hindlimb (Full and Ahn, 1995). Using a computer program (SIMM, Software for Interactive Musculoskeletal Modeling, MusculoGraphics, Inc) (Delp and Loan, 1995) and the kinematic variables measured during running, muscle strain for 177c and the strain patterns for 177c and 179 were determined (see Delp et al., 1990; Full and Ahn, 1995). Muscle strain is directly proportional to joint angle in insect legs because these muscles insert on apodemes (arthropod 'tendon'), which are 40 times stiffer than vertebrate tendon (Ker, 1977). Given the apodeme stiffness, the apodeme strains less than 0.01 % for the forces experienced by the muscles.

Muscle experiments

Animals were chilled and attached to a Lucite chamber using epoxy resin. Details of the apparatus were as described by Full et al. (1998). The Lucite chamber restrained the animal while the epoxy resin held the hindlimb fixed so that the coxa–femur joint angle was set at approximately 90 °. This joint angle was chosen to approximate the resting length for muscle 179 (104 %) (Full et al., 1998). We assumed that the resting length occurred at the same joint angle for muscle 177c. The dissection began with removal of the exoskeleton from the area of the metathoracic ganglion so that the connectives between thoracic ganglia 2 and 3 (i.e. the ventral nerve cord) could be severed. The resting length of the muscle was estimated before and after the experiment using an ocular micrometer and digital calipers. The dissected area was periodically moistened with insect Ringer's solution as required (Becht et al., 1960). Muscle cross-sectional area was determined from muscle mass and muscle length assuming a muscle density of 1 g cm^{-3}. Muscle forces were measured with a servo motor system (Cambridge Technology, Inc; model 300B) and recorded with a computer program (Labview, National Instruments) that controlled muscle length while measuring muscle force. A small hook on the lever arm held the muscle apodeme. The muscle was stimulated (Grass S48 stimulator) through the nerve (nerve 4 for muscle 177c and nerve 5 for muscle 179) using a suction electrode. The stimulation consisted of 0.5 ms square-wave pulses at approximately twice the threshold voltage. Trials were separated by 2 min intervals to minimize potentiation and fatigue. Maintenance of muscle performance was periodically checked with contractions generated by the *in vivo* stimulation pattern for each muscle (two or three muscle action potentials). The experiment was stopped when the amplitude of muscle contraction force declined by more than 10 % of its original force. The *in situ* muscle force measurements were all performed at 25 °C.

Muscle 177c was isolated by dissecting away the ventral

exoskeleton of the coxa and removing the other extensor muscles (179, 177a, 177e and 177d). It was particularly important to cut away muscle 177a because it inserts onto the same apodeme as 177c and is innervated by the same motor neuron as 177c. The trochanteral exoskeleton connected to the 177 apodeme was carefully cut, allowing the distal end of the muscle to attach to the lever arm (Fig. 1). To expose the distal end of muscle 179, we cut away a small area of the ventral exoskeleton of the coxa. The dissection to expose 179 was minimal because this muscle is the most superficial/ventral muscle in the group (Fig. 1). Tracheae or other muscles were not exposed. The trochanteral exoskeleton connected to the 179 apodeme was cut carefully, allowing the distal end of the muscle to be attached to the lever arm.

Isometric contractions

The semi-isolated muscle was stimulated through the nerve using a suction electrode, as described above. For isometric contractions, we used trains of 1–6 stimuli at a stimulation frequency of 100 pulses s^{-1}. Tetanic stimulation bursts consisted of 200 ms bursts at 200 pulses s^{-1}. Muscles were rested for 5–10 min after each tetanic stimulation.

Twitch kinetics included the time to peak force (T_{max}), time to 50 % relaxation (T_{50off}) and time to 90 % relaxation (T_{90off}). These times began with the onset of stimulation to represent most closely the time between muscle activation and force generation *in vivo* and, therefore, include the latency period or the time between the onset of stimulation and the onset of force.

Maximum shortening velocity

The maximum velocity of shortening was estimated by determining the force–velocity relationships of the muscles using the force-clamp method (Edman, 1979). Maximally stimulated muscles were allowed to shorten isotonically at different force levels. The velocity of shortening was determined for each force level. The maximum shortening velocity (V_{max}) for each muscle was determined using the least-squares method, which extrapolated the force–velocity measurements to zero force (Wohlfart and Edman, 1994). The muscles were rested for 5 min between trials unless the maximum tetanic force declined. If the maximum tetanic force declined by 5 % or more, then the experiment was stopped. The *in situ* contraction velocities for both muscles were filtered using a third-order, low-pass Butterworth filter with a cut-off frequency of 25 Hz.

Work loop method

Animals were mounted and muscles dissected as described above for isometric contractions. The *in vivo* conditions used to determine muscle work (muscle strain, phase, frequency and duration of stimulation) were obtained from the EMG/kinematics trials. The area of the third loop formed by plotting muscle force as a function of muscle length gave the work per cycle (Josephson, 1985a). Net *in vivo* power was calculated by dividing net *in vivo* work by the cycle period. To test the effects of small changes in phase and strain on muscle power output, we varied these parameters independently. While keeping the other *in vivo* conditions constant, the phase of stimulation onset was varied independently of strain, and strain was varied independently of the phase of stimulation. The force and stress results for muscle 179 were filtered using a third-order, low-pass Butterworth filter with a cut-off frequency of 50 Hz, because the lowest signal-to-noise ratio was 35:1, on average. Forces for 177c were not filtered because the signal-to-noise ratio was 300:1.

Statistical analyses

All data were calculated as the mean ± S.D. To avoid pseudo-replication, each animal generated a single data point for all data sets, unless a parameter was varied (e.g. strain amplitude, phase of stimulation). If there were duplicate data from any given animal under a single set of conditions, the values were averaged to represent that animal under that set of conditions. Groups of data were compared using the unpaired *t*-test to give *P*-values (StatView 5.0). Mann–Whitney *U*-tests were used to test for differences in activity patterns between the two muscles (StatView 5.0).

Results

In vivo *conditions during running*

Animals ran at speeds ranging from 13 to 30 cm s^{-1}, averaging 25±8 cm s^{-1} (*N*=6). The stride frequency ranged from 7 to 12 Hz (average 10 Hz), with a cycle duration of 106±19 ms.

Muscle 177c was activated after the beginning of joint extension (or muscle shortening). The activation began at a phase of 37.6±10.7 % (Fig. 2), where 0 and 100 % represent midway through joint flexion (or muscle lengthening) (Full et al., 1998). The number of muscle action potentials for 177c ranged from one to four per cycle, averaging 1.8±0.6. The interspike interval was 11±2 ms. Muscle 177c was activated for 7.3±6.2 % (or 7.3±6.8 ms; *N*=6) of each cycle.

Muscle 179 was also activated after the beginning of joint extension (or muscle shortening), but generally before 177c. The phase of activation was 25.7±7.1 % for muscle 179. The number of muscle action potentials for 179 ranged from two to four per cycle, averaging 2.7±0.5. The interspike interval was 11±7 ms. Muscle 179 was activated for 17.0±9.1 % (or 18.8±11.9 ms; *N*=6) of each cycle period.

The number of discrete muscle action potentials per burst differed between the two muscles during running (two muscle action potentials for 177c; three muscle action potentials for 179; *P*=0.01). Although the phase of burst onset differed for the two muscles (*P*=0.037), the bursts ended at the same phase of the cycle (offset phase 44.9±12.7 % for 177c; offset phase 42.7±6.1 % for 179; *P*=0.20). These patterns of onset and offset correspond to overlapping periods of activation of the two muscles during running (Fig. 2). Although the number of muscle action potentials differed with similar interspike intervals (*P*=0.76), the burst durations of the two muscles were

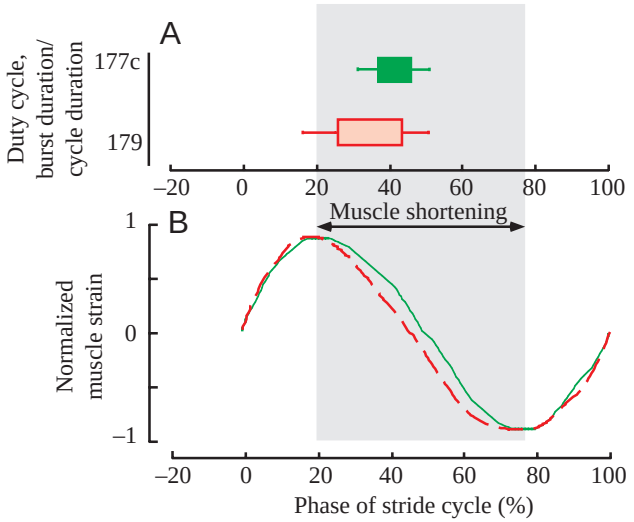

Fig. 2. EMG onset and duration relative to the running cycle. (A) EMG onset phases are represented by the start of the solid boxes and the left-hand error bars. The duty cycle (or burst duration normalized to cycle duration) was 7.3±6.2 % (*N*=6) for muscle 177c (green box) and 17.0±9.1 % (*N*=6; means ± S.D.) for muscle 179 (red box) and is represented by the length of the box and the right-hand error bars. The shaded region is the phase during which the extensors were shortening during the running cycle. (B) Normalized muscle strain plotted *versus* phase. Muscle length for each muscle, where 177c is represented by the solid line and 179 is represented by the dashed line, was normalized relative to its maximum and minimum lengths.

not statistically different (*P*=0.078). The burst duration normalized to stride period (i.e. duty cycle) of the two muscles were also similar (*P*=0.055). Variation in our sample size resulted in the paradox that the number of action potentials differed between the muscles, yet no difference could be resolved in interstimulus interval or burst duration. To characterize the activation pattern during running, we first selected the variable that showed the strongest statistical difference, the mean number of muscle action potentials per cycle (two for muscle 177c and three for 179). Next, we chose a constant interstimulus interval of 11 ms because we found no statistical difference between the muscles and this was exactly the interval measured previously for muscle 179 (Full et al., 1998). Finally, we selected the onset phase of the burst on the basis of the statistically significant difference between the muscles (38 % for muscle 177c and 26 % for 179).

The muscles shortened and lengthened cyclically with each stride during running. During the stance phase, the joint extended as the extensor muscles shortened. Conversely, during the swing phase, the muscles lengthened as the joint flexed. Total muscle strain over a stride during running was calculated as 7 % for muscle 177c (7.5±1.5 %; *N*=6) and 16.4±2.8 % (Full et al., 1998) for muscle 179.

Muscle properties

Isometric contraction kinetics

The rates of isometric force development and relaxation of single twitches did not differ between 177c and 179 (Table 1). The times to 90 % relaxation (T_{90off}) were approximately twice as long as the times to peak force (T_{max}) for both muscles.

The kinetics of isometric contractions differed when using the *in vivo* activation patterns (Table 1). However, this observed difference in the contraction kinetics reflects the difference in stimulation pattern (two *versus* three muscle action potentials per cycle) rather than a difference in the intrinsic characteristics of the muscles. Muscle 177c contracted and relaxed faster than 179, but only when stimulated with their *in vivo* activation patterns.

Force–velocity relationships

Both absolute and relative force–velocity relationships differed between the two muscles. Muscle 177c (mean length 8.95±0.47 mm; *N*=7; measured from the muscles that were

Table 1. *Isometric contraction kinetics of cockroach leg extensor muscles*

Activation pattern	Muscle	*N*	T_{max} (ms)	T_{50off} (ms)	T_{90off} (ms)	Latency (ms)	Stress (N cm^{-2})
Twitch	177c	10	27.6±2.9	39.8±6.0	53.2±7.9	10.0±0.3*	6.9±2.6 (*N*=6)
	179	8	26.5±4.8	39.5±6.2	60.2±7.6	8.9±0.9*	1.0±0.6
			P=0.54	*P*=0.55	*P*=0.08	*P*=0.001	
In vivo	177c	6	35.8±2.9*	47.9±4.0*	61.5±4.7*	10.1±0.3* (*N*=9)	12.8±3.6 (*N*=7)
	179	8	46.8±5.3*	61.7±7.6*	76.3±9.9*	9.0±0.8*	20.1±7.9
			P=0.0002	*P*=0.0021	*P*=0.0082	*P*=0.003	
Tetanus	177c	6					25.6±8.0
	179	8					47.2±8.9

Values are means ± S.D.

In vivo contraction kinetics for muscle 177c used two pulses of stimulation per cycle, *in vivo* contraction kinetics for muscle 179 used three pulses of stimulation per cycle.

* denotes a statistically significant difference (*P*<0.05; unpaired *t*-tests).

T_{max}, time to peak force; T_{50off}, time to 50 % relaxation; T_{90off}, time to 90 % relaxation; latency, time between the onset of stimulation and the onset of force.

used to determine *in vivo* power) was more than twice as long as muscle 179 (mean length 4.14±0.25 mm; *N*=6). The absolute, maximal rate of shortening of muscle 177c (49.2±6.7 mm s^{-1}; *N*=4) was much greater than that of muscle 179 (20.6±3.0 mm s^{-1}; *N*=4; Fig. 3A). However, once normalized for muscle length, the force–velocity relationships of 177c and 179 were more similar. The relative V_{max} for 177c (5.7±0.4 *L* s^{-1}; *N*=4, where *L* is muscle length), was greater than the relative V_{max} of 179 (4.9±0.4 *L* s^{-1}; *N*=4; *P*=0.02; Fig. 3B).

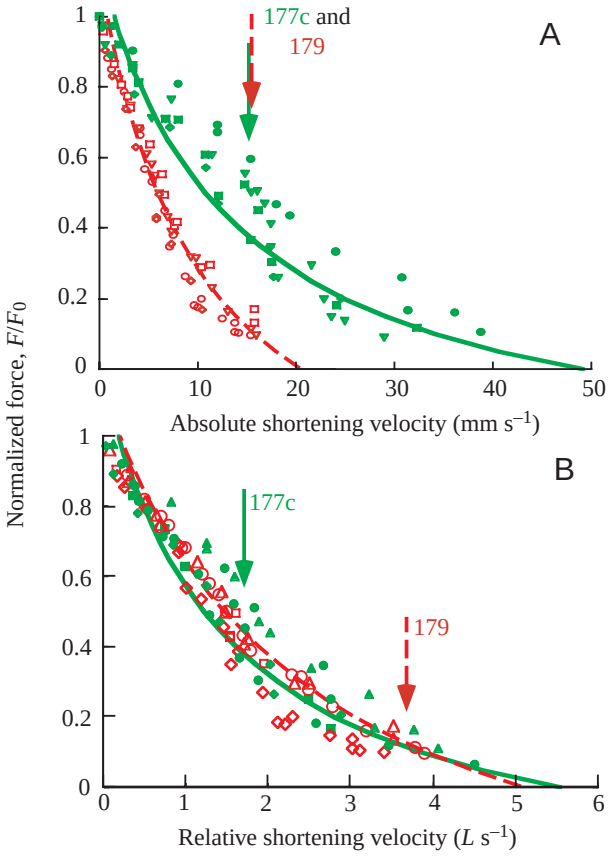

Fig. 3. The force–velocity relationships of maximally stimulated muscle (177c, 179) while shortening isotonically at different force levels. Both graphs represent the same data set, but are plotted with different abscissas. Each symbol represents a different animal (*N*=4 for each muscle). The filled symbols and solid line represent muscle 177c, whereas the open symbols and dashed line represent muscle 179. Force–velocity relationships were established for each individual (see text). The Hill coefficients were then averaged to obtain the overall force–velocity relationships for each muscle, represented by the lines. (A) Absolute force–velocity relationship. In absolute terms, the muscles shorten maximally at the same velocity during running (arrows; approximately 15 mm s^{-1}). (B) Relative force–velocity relationship. Muscle 177c was more than twice as long as muscle 179. Therefore, in relative terms, maximum shortening velocity, V_{max}, for muscle 177c was 5.7±0.4 *L* s^{-1} (*N*=4), where *L* is muscle length. The maximum *in situ* contraction velocity was approximately one-third V_{max} or 1.7±0.2 *L* s^{-1} (*N*=7; solid arrow) for 177c. V_{max} for muscle 179 was 4.9±0.4 *L* s^{-1} (*N*=4), while the maximum *in situ* relative contraction velocity of 179 was 3.7±0.1 *L* s^{-1} (*N*=6), which is near its V_{max} (dashed arrow). The Hill constants, which represent the curvature of the force–velocity relationship are *a*=0.5±0.3 and *b*=2.7±1.3 (*N*=4) for muscle 177c and *a*=0.6±0.2 and *b*=2.5±0.9 (*N*=4) for muscle 179. Values are means ± S.D.

Muscle stress and mechanical energy during simulated running

Although both muscles were activated during shortening (Fig. 4A–C), the two muscles generated force during different phases of running. *In vivo* conditions for 177c (8 Hz cycling frequency; two muscle action potentials at 100 pulses s^{-1}; onset stimulation phase 35 %; strain amplitude 7 %) resulted in the generation of muscle force during shortening (Fig. 4D). As the muscle lengthened, low passive force developed in muscle 177c, then declined before the end of lengthening (Fig. 4D). This pattern of force generation resulted in a larger, counterclockwise (positive work) loop with a smaller, clockwise tail (negative work) when force was plotted as a function of strain (Fig. 4E). The larger, counterclockwise loop indicates net power production from the muscle because force during shortening exceeded force during lengthening. Muscle 177c generated net positive power output (power 28.08±10.46 W kg^{-1}; work 3.51±1.31 J kg^{-1}; muscle mass 21.15±2.08 mg; *N*=7; Fig. 4E) in all the animals tested.

Unlike muscle 177c, muscle 179 generated very small forces during shortening and larger forces during lengthening under *in vivo* conditions (8 Hz cycling frequency; three muscle action potentials at 100 pulses s^{-1}; onset stimulation phase 28 %; strain amplitude 16.4 %). This pattern of force generation resulted in a clockwise (negative) work loop (Fig. 4D), which represents the absorption of net mechanical energy by muscle 179 under *in vivo* conditions. All 179 muscles operating under *in vivo* strain and stimulation conditions performed net negative work (power –19.13±14.09 W kg^{-1}; work –2.39±1.76 J kg^{-1}; muscle mass 3.19±0.52 mg; *N*=6; Fig. 4E). Although most of the energy absorbed by muscle 179 was passive (approximately 80 %), the imposed *in vivo* stimulation pattern caused more energy to be absorbed by each muscle than when cycled passively (*N*=4; *P*<0.05; paired *t*-test). These data for muscle 179 agree well with previously published data on the same muscle (179) from the same species (*Blaberus discoidalis*) (Full et al., 1998). Although all the muscles measured absorbed net energy, the shapes of the work loops varied, also as previously reported (Full et al., 1998). The shapes of the work loops fell into two main categories. Most muscles generated the highest forces at the end of muscle lengthening (as shown in Fig. 4E) and one muscle generated the highest forces at the beginning of muscle lengthening.

Muscle strain

We used muscle strains of 7 % for muscle 177c and 16.4 % for muscle 179 to determine the work done by the muscles under *in vivo* conditions. To ensure that our conclusions would

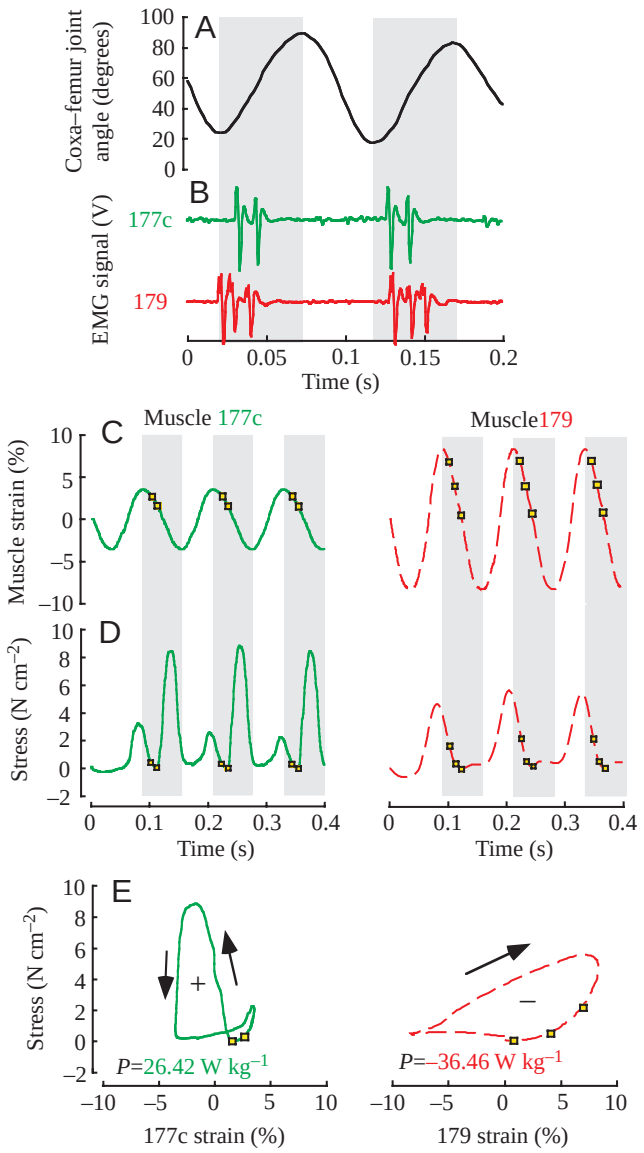

Fig. 4. Function of muscles 177c and 179 during the preferred-speed running. (A,B) Simultaneous coxa–femur joint kinematics of the hindlimb and EMG recordings of muscles 177c and 179 during preferred-speed running. The coxa–femur joint angle increased with extension during stance (shaded areas) and decreased with flexion. Both muscles were activated during shortening. Note the overlap in muscle activity. (C,D) Individual muscle strain and stress during isolated muscle experiments. The shortening and lengthening patterns were determined from the joint kinematics during running. Muscle forces were measured as the muscles were stimulated to simulate preferred-speed running. (E) Work loops generated using *in vivo* conditions. The counterclockwise direction of the muscle 177c work loop illustrates that this muscle generated higher forces during shortening than during lengthening, resulting in positive work or power output (*P*). The clockwise direction of the work loop for muscle 179 illustrates that this muscle generated higher forces during lengthening than during shortening, resulting in negative work or energy absorption when operating under preferred-speed running conditions. The shaded areas indicate the stance phase of running when the joint angle increases and the muscles shorten. Squares represent the timing of muscle action potentials.

not be affected by errors in strain measurement, we tested the sensitivity of muscle power output to strain amplitude. Muscle 177c always generated net positive power over the range of muscle strains (5.7–8.4 %; *N*=6; Fig. 5) used during running (stimulation phase 35 %; two muscle action potentials per cycle; Fig. 5). Muscle 179 always absorbed net energy over the range of strains (14–18.5 %; *N*=6) used under *in vivo* conditions (stimulation phase 28 %; three muscle action potentials per cycle; Fig. 5).

Stimulation onset phase

To examine the sensitivity of muscle power to stimulation phase, we varied the phase of stimulus onset for each muscle, while holding the other *in vivo* parameters constant (e.g. strain amplitude and burst duration). Muscle power output varied with stimulation phase in both muscles. Muscle 177c generated maximum power output when stimulated at the beginning of the shortening phase (Fig. 6). As phase increased, so that stimulation began later during the shortening phase, the power generated by muscle 177c decreased. When stimulated midway through shortening (phase 42 %), muscle 177c neither generated nor absorbed mechanical energy over a cycle. Although we did not measure power output from muscle 177c at phases greater than 42 %, the trend clearly indicated that this muscle would absorb energy when stimulated during the latter half of shortening. In contrast, when muscle 179 was stimulated during the latter half of lengthening (phase 0–20 %), it generated positive power. However, power decreased in muscle 179 as phase increased. When stimulated any time during shortening or during the first half of lengthening (phase 20–95 %), muscle 179 absorbed net mechanical energy.

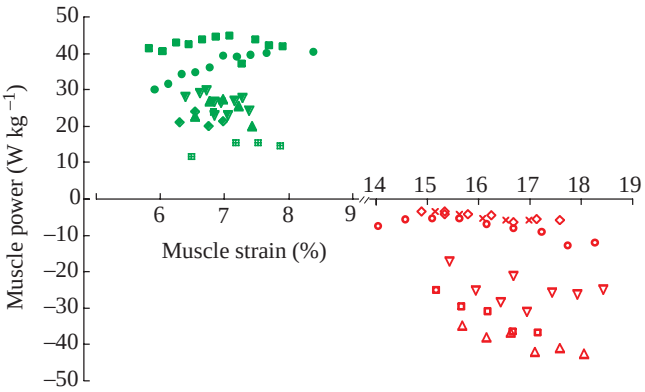

Fig. 5. Muscle power as a function of strain. Each symbol represents a different animal. The closed green symbols represent muscle 177c. Muscle 177c always generated power when operating over a range of strain amplitudes near its *in vivo* strain (7 %). The open red symbols represent muscle 179. Muscle 179 always absorbed energy when operating over a range of strain amplitudes near its *in vivo* running strain (16.4 %). Muscle function was not sensitive to strain excursion (or joint angle amplitude) when operating under otherwise *in vivo* running conditions.

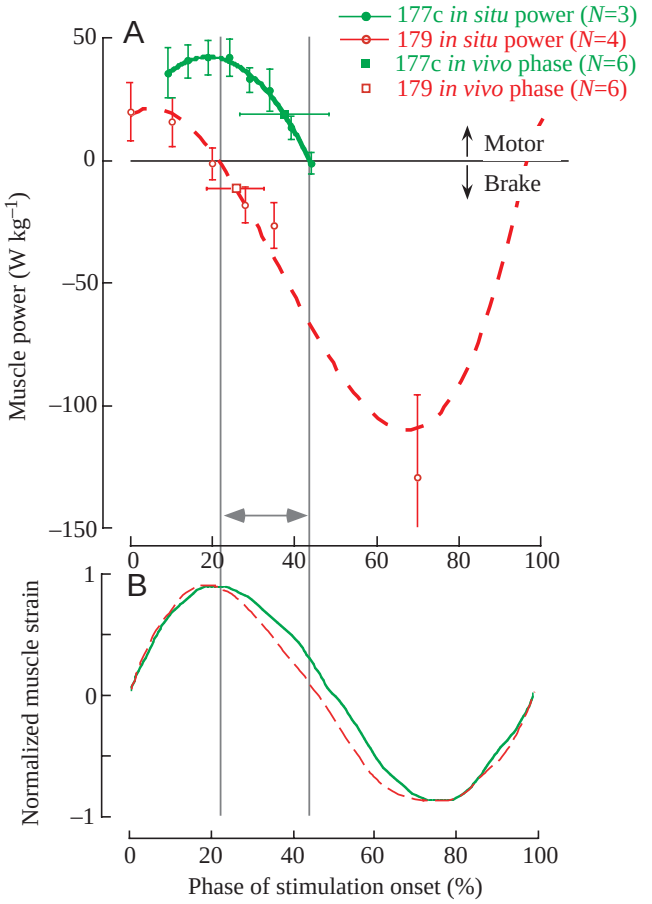

Fig. 6. Muscle power output as a function of the phase of stimulation onset for muscles 177c and 179. (A) Muscle power for both muscles relative to the phase of stimulation onset. Muscle power varied as a function of stimulation onset phase for both muscles. The stimulation onset phase at which power peaks differed for the two muscles. The region within the vertical lines indicated by the double-headed arrow represents the range of stimulus onset phase within which muscle 177c performed positive work while muscle 179 absorbed mechanical energy. Within these lines, muscle 177c always functioned as a power generator when operating under preferred-speed running conditions (two muscle action potentials per cycle; 8 Hz cycle frequency). Muscle 179 always functioned as an energy absorber when operating under preferred-speed running conditions (three muscle action potentials per cycle; 8 Hz cycle frequency). The filled green (177c) and open red (179) symbols represent the measured mean onset phases during running, including standard deviations. (B) Normalized muscle strain plotted *versus* phase. Muscle length for each muscle, where 177c is represented by the green line and 179 is represented by the red line, was normalized relative to its maximum and minimum lengths.

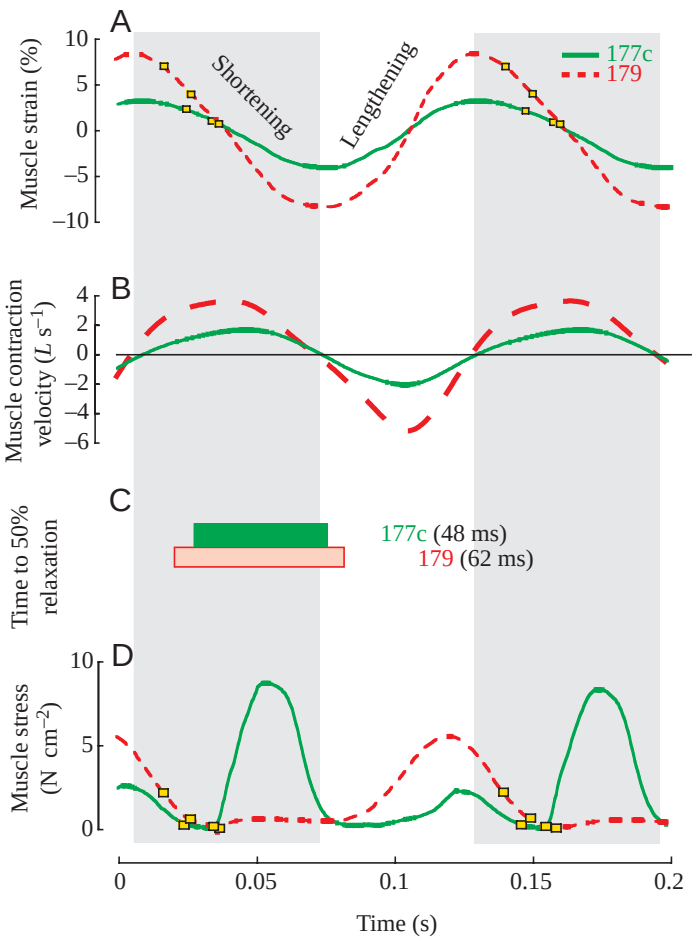

Fig. 7. Muscle strain, contraction velocity, contraction duration, and *in situ* force generation for muscles 177c and 179 as a function of time. (A) Muscle 179 (dashed lines) underwent larger strain amplitudes because it is shorter than 177c (solid lines). (B) Because both muscles cycled at (8 Hz) during running, 179 experienced faster shortening and lengthening velocities than the longer 177c. (C) Contraction duration is represented by the time to 50 % relaxation. During running, muscle 179 was stimulated for longer (three muscle action potentials at 100 pulses s^{-1}) than 177c (two muscle action potentials at 100 pulses s^{-1}) and thus 179 generated force for longer. (D) Muscle 177c generated force during muscle shortening and relaxed before the muscle began to lengthen. Muscle 179, however, generated lower levels of force during shortening, possibly because it shortened at very high velocities. Muscle 179 began generating force as the contraction velocity slowed and approached zero. Muscle 179 was still active as the muscle lengthened, when it generated its highest forces, resulting in net negative work during the running cycle. The shaded areas indicate the stance phase of running when the muscles shorten. Yellow squares represent the timing of muscle action potentials.

Discussion

Differential muscle function during locomotion

Contrary to the accepted hypothesis of synergy or load-sharing, muscles capable of executing the same action at a common joint can function differently during locomotion. Different muscles that appear redundant within a group can serve different roles within the same cycle of leg movement. In the present study, we demonstrated that one leg extensor (177c) operated like a motor, producing mechanical energy to extend the hindlimb actively at the coxa–femur joint, while another leg extensor (179) actively absorbed mechanical energy to slow flexion, stabilize the joint, and/or resist

perturbations during running. This differential function occurred in two muscles that do not appear to differ substantially in anatomical arrangement or activation pattern. Both extensor muscles were activated by action potential bursts that overlap during the first half of shortening. Both muscles comprise a single motor unit (Pipa and Cook, 1959). Homologues of both muscles are histochemically classified as fast-twitch muscles in the American cockroach *Periplaneta americana* (Stokes et al., 1979; Morgan et al., 1980). To understand the factors that contribute to the difference in mechanical function between the two muscles, we needed to compare their contraction kinetics, shortening velocities and neural control.

Twitch kinetics

Twitch kinetics (times to peak force, 50 % relaxation, and 90 % relaxation) did not explain why one muscle (177c) generated energy and the other (179) absorbed energy during running. The twitch kinetics were similar between muscles 177c and 179 (Table 1). For both muscles, twitch duration (i.e. time to 50 % relaxation) lasted less than half the stride period (62.5 ms at 8 Hz stride frequency). A twitch duration shorter than half the stride period suggests that the muscle has the capacity to produce power during running because it could generate force during the shortening phase and then relax before lengthening begins.

In vivo *contraction velocities*

Strain rate and amplitude can also influence a muscle's ability to generate force and produce power (Josephson, 1985a; Josephson and Stokes, 1989; Marsh, 1999). Muscles generate maximum power output at approximately one-third V_{max} in fish (Curtin and Woledge, 1988; Rome et al., 1988), mammals (Syme and Stevens, 1989; James et al., 1996; Swoap et al., 1997), frogs (Stevens, 1988) and crabs (Josephson and Stokes, 1989). However, if the muscle shortens quickly, near its V_{max}, then the positive work done by the muscle during shortening may not exceed the work needed to re-lengthen the muscle. Therefore, a muscle shortening near V_{max} during cyclic contractions may not generate positive power (Josephson, 1985b; Josephson and Stokes, 1989). The strain rate of a muscle depends on the length of its moment arm (r) and the angular velocity of the joint. Because muscles 177c and 179 operate at the same joint and have similar mean moment arms (r=0.76 mm for 177c; r=0.54 mm for 179) (Full and Ahn, 1995), they shorten at similar absolute velocities (maximum *in situ* velocity approximately 15 mm s^{-1}; Fig. 3A). However, muscle 177c was approximately twice as long as muscle 179, thus shortening relatively half as fast as 179. The greatest relative *in situ* shortening velocity for muscle 177c was only 1.7 L s^{-1}, whereas muscle 179 shortened more than twice as fast (3.7 L s^{-1}; Fig. 7B). Although the two muscles contracted at the same peak absolute velocities, they operated on different regions of their relative force–velocity relationships (Fig. 3B). The longer, relatively slower-contracting muscle (177c) operated near one-third V_{max} (1.75 L s^{-1}), the relative velocity at which isotonic power is maximized. In contrast, the shorter muscle (179) shortened near its V_{max} (Fig. 3B), resulting in very little force production during shortening (Fig. 7B,D). These differences in relative shortening velocities largely account for the observed differences in muscle performance during running.

Force–velocity effects, caused by different muscle lengths, contribute to the difference in maximum power output between muscles 177c and 179 (Fig. 6). At phases that result in maximum power output (9–19 %), muscle 177c generated substantial forces during shortening, even when shortening velocities were high. At these same phases, muscle 179 shortened relatively faster to generate lower forces during shortening, thereby producing lower power outputs (Fig. 6A). This difference in relative shortening velocity accounts for the greater magnitude of maximum, mass-specific power generated by muscle 177c compared with muscle 179.

History-dependent effects: force depression due to active shortening

Force depression due to active shortening of muscle is another intrinsic property that is influenced by muscle strain and determines force and work output. Shortening-induced force depression reduces the work and power output of muscles undergoing large strains during cyclic contractions (Edman, 1975; Josephson, 1997; Askew and Marsh, 1998; Josephson and Stokes, 1999). Moreover, force depression induced by active shortening increases with increasing strain (Edman, 1975). This effect may further depress the force generated by muscle 179 during shortening (Fig. 7D). Muscle 179 experiences greater strain amplitudes (16.4 %) than muscle 177c (7 %) and, therefore, would be expected to experience greater force depression than muscle 177c (Edman, 1975). When stimulated at the beginning of shortening or later, muscle 179 only absorbed energy over the cycle (Fig. 6A; phase >20 %), while this muscle generated power when stimulated before shortening (phase <20 %). When stimulated during shortening (phase >20 %), the force of muscle 179 may be depressed as a result of active shortening. This phenomenon probably depressed force in muscle 177c as well, but to a lesser degree because it experienced smaller strain amplitudes. The difference in force depression due to active shortening between the muscles may contribute to the difference in mechanical performance of the muscles during running.

Integration of neural control and muscle mechanics

A major determinant of muscle power output during cyclical contractions is the phase of stimulation (Josephson, 1985a, 1999). As expected, the function of muscles 177c and 179 varied with stimulation phase (Fig. 6). When stimulated before shortening (phase <20 %), both muscles functioned as motors. When stimulated between the beginning of shortening and mid-shortening (phase 20–40 %), the two muscles functioned differently, even when stimulated at the same phase. When stimulated after mid-shortening (phase >40 %), both muscles

absorbed mechanical energy. Under *in vivo* conditions during running, the animal generally activated muscle 177c when this muscle generated mechanical energy while activating 179 at phases at which this muscle absorbed mechanical energy (Fig. 6).

The similarity in twitch kinetics would not predict differences in mechanical function if the animal activated the muscles by single muscle action potentials. Differences in contraction kinetics due to differences in muscle action potential number did, however, offer a partial explanation of how one muscle functioned as a motor and the other as a brake. With their *in vivo* stimulation patterns, muscle 177c contracted and relaxed faster than 179 (Table 1). Within a cycle, muscle 177c generated force during shortening and then relaxed before lengthening began. In contrast, on the basis of the duration of activation predicted from isometric contractions, muscle 179 remained active throughout shortening and through part of lengthening (Fig. 7). However, the kinetics of isometric force development provide only a first approximation of how long a muscle can generate force when contracting isometrically and do not provide sufficient information to predict muscle function during locomotion.

Although the simplest assumption concerning the operation of a multiple muscle system is that of synergy or equal load-sharing, we show that muscles within a muscle group do not necessarily manage energy similarly during running. Individual muscles within the same anatomical muscle group can function as power-generating motors (177c) or as energy-absorbing dampers (179) during running. Anatomy, muscle activation patterns, kinematics, twitch kinetics or isotonic force–velocity measurements alone may be insufficient to predict *in vivo* muscle function. Muscle function depends on the dynamic interactions between a large number of variables (Josephson, 1999). Without the direct determination of muscle forces under *in vivo* stimulation and strain conditions, predicting *in vivo* muscle function during locomotion can be difficult, if not impossible. Depending on activation pattern, contraction velocity and history-dependent effects under the *in vivo* strain and stimulation conditions, apparent redundancy within a multiple muscle group may instead represent diversity in muscle function.

We thank D. Stokes and R. Josephson for support and assistance in setting up our equipment, Ed Chen for assistance in data collection and analysis, C. Farley and M. Koehl for discussions of the experiments and careful comments on the manuscript and K. Meijer, S. Lehman and the Berkeley Biomechanics Group (especially D. Jindrich, Y. H. Chang, T. Griffin and C. Shigeoka) for comments on earlier versions of the manuscript. The authors are indebted to the anonymous reviewers for their helpful comments. This research was supported by ONR Grant N00014-92-J-1250 AASERT Award and Sigma Xi Grants-In-Aid of Research and Department of Integrative Biology Summer Fellowship to A.N.A. and ONR Grant N00014-92-J-1250 and ONR Grant MURI N00014-98-1-0669 to R.J.F.

References

Abraham, L. D. and Loeb, G. E. (1985). The distal hindlimb musculature of the cat. *Exp. Brain Res.* **58**, 580–593.

Altringham, J. D., Wardle, C. S. and Smith, C. I. (1993). Myotomal muscle function at different locations in the body of a swimming fish. *J. Exp. Biol.* **182**, 191–206.

Askew, G. N. and Marsh, R. L. (1998). Optimal shortening velocity (V/V_{max}) of skeletal muscle during cyclical contractions: length–force effects and velocity-dependent activation and deactivation. *J. Exp. Biol.* **201**, 1527–1540.

Becht, G., Hoyle, G. and Usherwood, P. N. R. (1960). Neuromuscular transmission in the coxal muscles of the cockroach. *J. Insect Physiol.* **4**, 191–201.

Biewener, A. A., Dial, K. P. and Goslow, G. E., Jr (1992). Pectoralis muscle force and power output during flight in the starling. *J. Exp. Biol.* **164**, 1–18.

Biewener, A. A. and Full, R. J. (1992). Force platform and kinematic analysis. In *Biomechanics – Structures and Systems: A Practical Approach* (ed. A. A. Biewener), pp. 45–96. New York: Oxford University Press.

Biewener, A. A. and Gillis, G. B. (1999). Dynamics of muscle function during locomotion: accommodating variable conditions. *J. Exp. Biol.* **202**, 3387–3396.

Biewener, A. A., Konieczynski, D. D. and Baudinette, R. V. (1998). *In vivo* muscle force–length behavior during steady-speed hopping in tammar wallabies. *J. Exp. Biol.* **201**, 1681–1694.

Caiozzo, V. J. and Baldwin, K. M. (1997). Determinants of work produced by skeletal muscle: potential limitations of activation and relaxation. *Am. J. Physiol.* **273**, C1049–C1056.

Carbonell, C. S. (1947). The thoracic muscles of the cockroach *Periplaneta americana*. *Smithson. Misc. Collns* **107**, 1–23.

Coughlin, D. J., Zhang, G. and Rome, L. C. (1996). Contraction dynamics and power production of pink muscle of the scup (*Stenotomus chrysops*). *J. Exp. Biol.* **199**, 2703–2713.

Crowninshield, R. D. (1978). Use of optimization techniques to predict muscle forces. *J. Biomech. Engng.* **100**, 88–92.

Curtin, N. A. and Woledge, R. C. (1988). Power output and force–velocity relationship of live fibres from white myotomal muscle of the dogfish *Scyliorhinus canicula*. *J. Exp. Biol.* **140**, 187–197.

Davy, D. T. and Audu, M. L. (1987). A dynamic optimization technique for predicting muscle forces in the swing phase of gait. *J. Biomech.* **20**, 187–201.

Delp, S. L. and Loan, J. P. (1995). A graphics-based software system to develop and analyze models of musculoskeletal structures. *Comp. Biol. Med.* **25**, 21–34.

Delp, S. L., Loan, J. P., Hoy, M. G., Zajac, F. E., Topp, E. L. and Rosen, J. M. (1990). An interactive graphics-based model of the lower extremity to study orthopaedic surgical procedures. *IEEE Trans. Biomed. Eng.* **37**, 757–767.

Dickinson, M. H., Farley, C. T., Full, R. J., Koehl, M. A. R., Kram, R. and Lehman, S. (2000). How animals move: an integrative view. *Science* **288**, 100–106.

Dul, J., Townsend, M. A., Shiavi, R. and Johnson, G. E. (1984). Muscular synergism. I. On criteria for load sharing between synergistic muscles. *J. Biomech.* **17**, 663–673.

Edman, K. A. P. (1975). Mechanical deactivation induced by active shortening in isolated muscle fibres of the frog. *J. Physiol., Lond.* **246**, 255–275.

Edman, K. A. P. (1979). The velocity of unloaded shortening and its relation to sarcomere length and isometric force in vertebrate muscle fibres. *J. Physiol., Lond.* **291**, 143–159.

Fourtner, C. F. and Randall, J. B. (1982). Studies on cockroach flight: The role of continuous neural activation of non-flight muscles. *J. Exp. Zool.* **221**, 143–154.

Full, R. J. and Ahn, A. N. (1995). Static forces and moments generated in the insect leg: comparison of a three-dimensional musculo-skeletal computer model with experimental measurements. *J. Exp. Biol.* **198**, 1285–1298.

Full, R. J., Stokes, D. S., Ahn, A. N. and Josephson, R. K. (1998). Energy absorption during running by leg muscles in a cockroach. *J. Exp. Biol.* **201**, 997–1012.

Gregor, R. J., Roy, R. R., Whiting, W. C., Lovely, R. G., Hodgson, J. A. and Edgerton, V. R. (1988). Mechanical output of the cat soleus during treadmill locomotion: *In vivo* vs. *in situ* characteristics. *J. Biomech.* **21**, 721–732.

Herzog, W. and Leonard, T. R. (1991). Validation of optimization models

that estimate the forces exerted by synergistic muscles. *J. Biomech.* **24 (Suppl. 1)**, 31–39.

James, R. S., Altringham, J. D. and Goldspink, D. F. (1995). The mechanical properties of fast and slow skeletal muscles of the mouse in relation to their locomotory function. *J. Exp. Biol.* **198**, 491–502.

James, R. S., Young, I. S., Cox, V. M., Goldspink, D. F. and Altringham, J. D. (1996). Isometric and isotonic muscle properties as determinants of work loop power output. *Pflügers Arch.* **432**, 767–774.

Johnson, T. P., Swoap, S. J., Bennett, A. F. and Josephson, R. K. (1993). Body size, muscle power output and limitations on burst locomotor performance in the lizard *Dipsosaurus dorsalis*. *J. Exp. Biol.* **174**, 199–213.

Johnston, I. A. (1991). Muscle action during locomotion: a comparative perspective. *J. Exp. Biol.* **160**, 167–185.

Josephson, R. K. (1985a). Mechanical power output from striated muscle during cyclic contractions. *J. Exp. Biol.* **114**, 493–512.

Josephson, R. K. (1985b). The mechanical power output of a tettigoniid wing muscle during singing and flight. *J. Exp. Biol.* **117**, 357–368.

Josephson, R. K. (1993). Contraction dynamics and power output of skeletal muscle. *Annu. Rev. Physiol.* **55**, 527–546.

Josephson, R. K. (1997). Power output from a flight muscle of the bumblebee *Bombus terrestris*. II. Characterization of the parameters affecting power output. *J. Exp. Biol.* **200**, 1227–1239.

Josephson, R. K. (1999). Dissecting muscle power output. *J. Exp. Biol.* **202**, 3369–3375.

Josephson, R. K. and Stokes, D. R. (1989). Strain, muscle length and work output in crab muscle. *J. Exp. Biol.* **145**, 45–61.

Josephson, R. K. and Stokes, D. R. (1999). Work-dependent deactivation of a crustacean muscle. *J. Exp. Biol.* **202**, 2551–2565.

Ker, R. F. (1977). Some structural and mechanical properties of locust and beetle cuticle. PhD thesis, University of Oxford.

Kram, R., Wong, B. and Full, R. J. (1997). Three-dimensional kinematics and limb kinetic energy of running cockroaches. *J. Exp. Biol.* **200**, 1919–1929.

Lieber, R. L. and Brown, C. G. (1992). Sarcomere length–joint angle relationships of seven frog hindlimb muscles. *Acta Anat.* **145**, 289–295.

Marsh, R. L. (1990). Deactivation rate and shortening velocity as determinants of contractile frequency. *Am. J. Physiol.* **259**, R230–R233.

Marsh, R. L. (1999). How muscles deal with real-world loads: the influence of length trajectory on muscle performance. *J. Exp. Biol.* **202**, 3377–3385.

Marsh, R. L., Olson, J. M. and Guzik, S. K. (1992). Mechanical performance of scallop adductor muscle during swimming. *Nature* **357**, 411–413.

Morgan, C. R., Tarras, M. S. and Stokes, D. R. (1980). Histochemical demonstration of enzymatic heterogeneity within the mesocoxal and metacoxal muscles of *Periplaneta americana*. *J. Insect Physiol.* **26**, 481–486.

Pearson, K. G. and Iles, J. F. (1971). Innervation of coxal depressor muscles in the cockroach *Periplaneta americana*. *J. Exp. Biol.* **54**, 215–232.

Pipa, R. L. and Cook, E. F. (1959). Studies on the hexapod nervous system. I. The peripheral distribution of the thoracic nerves of the adult cockroach, *Periplaneta americana*. *Ann. Ent. Soc. Am.* **52**, 695–710.

Prilutsky, B. I., Herzog, W. and Allinger, T. L. (1996). Mechanical power and work of cat soleus, gastrocnemius and plantaris muscles during functional locomotion: possible function significance of muscle design and force patterns. *J. Exp. Biol.* **199**, 801–814.

Roberts, T. J., Marsh, R. L., Weyand, P. G. and Taylor, C. R. (1997). Muscular force in running turkeys: The economy of minimizing work. *Science* **275**, 1113–1115.

Rome, L. C., Funke, R. P., Alexander, R. McN., Lutz, G., Aldridger, H., Scott, F. and Freadman, M. (1988). Why animals have different muscle fibre types. *Nature* **335**, 824–827.

Rome, L. C., Swank, D. and Corda, D. (1993). How fish power swimming. *Science* **261**, 340–343.

Seireg, A. and Arvikar, R. J. (1975). The prediction of muscular load sharing and joint forces in the lower extremities during walking. *J. Biomech.* **8**, 89–102.

Stevens, E. D. (1988). Effect of pH and stimulus phase on work done by isolated frog sartorius muscle during cyclical contraction. *J. Muscle Res. Cell Motil.* **9**, 329–333.

Stokes, D. R., Vitale, A. J. and Morgan, C. R. (1979). Enzyme histochemistry of the mesocoxal muscles of *Periplaneta americana*. *Cell Tissue Res.* **198**, 175–189.

Swank, D. M., Zhang, G. and Rome, L. C. (1997). Contraction kinetics of red muscle in scup: mechanism for variation in relaxation rate along the length of the fish. *J. Exp. Biol.* **200**, 1297–1307.

Swoap, S. J., Caiozzo, V. J. and Baldwin, K. M. (1997). Optimal shortening velocities for *in situ* power production of rat soleus and plantaris muscles. *Am. J. Physiol.* **273**, C1047–C1063.

Swoap, S. J., Johnson, T. P., Josephson, R. K. and Bennett, A. F. (1993). Temperature, muscle power output and limitations on burst locomotor performance of the lizard *Dipsosaurus dorsalis*. *J. Exp. Biol.* **174**, 185–197.

Syme, D. A. and Stevens, E. D. (1989). Effect of cycle frequency and excursion amplitude on work done by rat diaphragm muscle. *Can. J. Physiol. Pharmacol.* **67**, 1294–1299.

Tu, M. S. and Dickinson, M. H. (1994). Modulation of negative work output from a steering muscle of the blowfly *Calliphora vicina*. *J. Exp. Biol.* **192**, 207–224.

Van Leeuwen, J. L., Lankheet, M. J. M., Asker, H. A. and Osse, J. W. M. (1990). Function of red axial muscles of carp (*Cyprinus carpio*): recruitment and normalized power output during swimming in different modes. *J. Zool. Lond.* **220**, 123–145.

Walmsley, B., Hodgson, J. A. and Burke, R. E. (1978). Forces produced by medial gastrocnemius and soleus muscles during locomotion in freely moving cats. *J. Neurophysiol.* **41**, 1203–1216.

Wohlfart, B. and Edman, K. A. P. (1994). Rectangular hyperbola fitted to muscle force–velocity data using three-dimensional regression analysis. *Exp. Physiol.* **79**, 235–239.